Characterization of the proteasome interaction network using a QTAX-based tag-team strategy and protein interaction network analysis

Cortnie Guerrero*, Tijana Milenković†, Nataša Pržulj†, Peter Kaiser‡, and Lan Huang*§

*Departments of Physiology and Biophysics and Developmental and Cell Biology, ‡Biological Chemistry, and †Computer Science,University of California, Irvine, CA 92697

Edited by Michael Rosbash, Brandeis University, Waltham, MA, and approved July 2, 2008 (received for review February 26, 2008)

Quantitative analysis of tandem-affinity purified cross-linked (*x*) protein complexes (QTAX) is a powerful technique for the identification of protein interactions, including weak and/or transient components. Here, we apply a QTAX-based tag-team mass spectrometry strategy coupled with protein network analysis to acquire a comprehensive and detailed assessment of the protein interaction network of the yeast 26S proteasome. We have determined that the proteasome network is composed of at least 471 proteins, significantly more than the total number of proteins identified by previous reports using proteasome subunits as baits. Validation of the selected proteasome-interacting proteins by reverse copurification and immunoblotting experiments with and without cross-linking, further demonstrates the power of the QTAX strategy for capturing protein interactions of all natures. In addition, >80% of the identified interactions have been confirmed by existing data using protein network analysis. Moreover, evidence obtained through network analysis links the proteasome to protein complexes associated with diverse cellular functions. This work presents the most complete analysis of the proteasome interaction network to date, providing an inclusive set of physical interaction data consistent with physiological roles for the proteasome that have been suggested primarily through genetic analyses. Moreover, the methodology described here is a general proteomic tool for the comprehensive study of protein interaction networks.

in vivo cross-linking | quantitative mass spectrometry

It has been estimated that every major process in the cell is carried out by assemblies of at least 10 proteins (1). Ideally, these protein assemblies work together in a highly regulated manner to maintain cellular homeostasis. However, aberrations in protein interaction networks can lead to various disease states. To aid in future drug development that targets interactions at the protein level, it is necessary to understand the regulatory mechanisms of each cellular process, including the identification of all proteins involved in these processes.

One of the many processes critical for cell function is the ubiquitin (Ub)-mediated degradation of proteins by the 26S proteasome. This degradation pathway regulates the intracellular levels of proteins involved in a wide variety of cellular functions including growth, cell cycle, transcription, apoptosis, DNA repair, and stress response (2). The 26S proteasome is a macromolecular complex of ≈2.5 MDa containing a catalytic core particle (CP), the 20S, which is capped on each side by a 19S regulatory particle (RP). The 20S CP is composed of two copies each of 14 subunits: 7α and 7β. The α and β subunits form four heptameric ring-like structures in the order of $\alpha\beta\beta\alpha$. The proteolytic activity of the proteasome is carried out by three β subunits, β1, β2, and β5. The 19S RP is composed of at least 20 different subunits, comprising two subcomplexes: a base containing six ATPases and two non-ATPase subunits and a lid containing at least 12 non-ATPase subunits (2, 3). Evidence suggests that the subunits of the RP play critical roles in the degradation process by interacting directly with incoming substrates, removing the Ub chain, and unfolding them before transfer into the 20S core for degradation.

Ub-mediated degradation by the 26S proteasome is a highly regulated process involving the concerted effort of the subunits of the CP and RP and many proteasome-interacting proteins (PIPs). In recent years, an increasing number of PIPs have been identified (4–8). One class of PIPs that have been the subject of numerous biochemical studies consists of the Ub receptor proteins. These proteins, such as yeast Rad23, Dsk2, and Ddi1, bind to substrates and then transfer them to the proteasome (3). It has also been suggested that substrates can be shuttled to the proteasome in a multistep process, which involves several PIPs, including the $Cdc48^{UFD1/NPL4}$ complex and Rad23/Dsk2. Despite intensive studies, the identification of other key components involved in this pathway remains limited. Thus, comprehensive profiling of the proteasome interaction network is required for the complete understanding of the mechanisms of the degradation process.

Native affinity purification combined with MS has successfully identified all of the known subunits of the yeast 26S proteasome and many PIPs (4, 5). Recently, tandem affinity purification (TAP)-MS has been applied to capture and identify yeast protein complexes at the proteome level (9–12). Interestingly, none of the approaches were able to capture all of the known Ub receptor proteins, Rad23, Dsk2, Ddi1, and the shuttling factor Cdc48 with the proteasome, likely due to the weak and transient nature of their interactions. Because these affinity-based purifications are carried out under native conditions, it is extremely difficult to preserve weak and/or transient interactions due to the necessity of various washing procedures.

To capture and identify specific PIPs, including stable, weak, and/or transient ones, we previously developed an integrated approach using *in vivo* chemical cross-linking of protein complexes and TAP under fully denaturing conditions [referred to as quantitative analysis of tandem-affinity purified cross-linked (*x*) protein complexes (QTAX)] (6). This strategy has been successfully used to map the yeast proteasome-interaction network using a histidine-biotin-histidine (HBH)-tagged proteasome subunit, i.e., Rpn11-HBH. Because the 26S proteasome is a large protein complex with >30 subunits, we suspect that tagging subunits at different positions in the proteasome assembly will increase the amount of interacting proteins identified. To obtain a more complete proteasome interaction network, we have therefore extended the QTAX strategy by incorporating a tag-team approach in this work. In addition,

Author contributions: C.G. and L.H. designed research; C.G. performed research; N.P. and P.K. contributed new reagents/analytic tools; C.G., T.M., N.P., and L.H. analyzed data; and C.G. and L.H. wrote the paper.

The authors declare no conflict of interest.

This article is a PNAS Direct Submission.

§To whom correspondence should be addressed. E-mail: lanhuang@uci.edu.

This article contains supporting information online at www.pnas.org/cgi/content/full/0801870105/DCSupplemental.

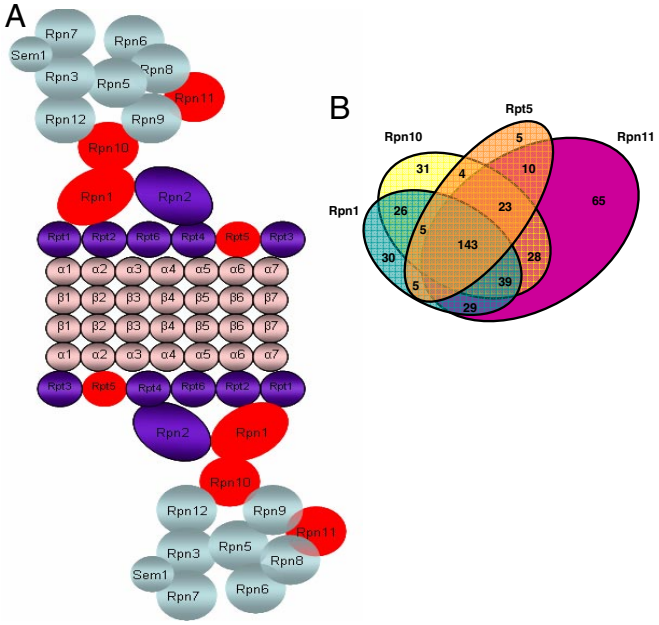

Fig. 1. Identifying PIPs using a QTAX-based tag-team strategy. (*A*) Illustration of the yeast 26S proteasome. Subunits in red (Rpn11, Rpn1, Rpn10, and Rpt5) were chosen for HBH tagging. (*B*) Comparison of the number of PIPs (SILAC ratios >1.5) captured by each bait.

changes in the sample preparation strategy have been implemented for increased protein identification and quantification. Moreover, protein interaction network analysis has been used to link the identified PIPs within the proteasome interaction network while providing a further understanding of the proteasome's role in various cellular pathways.

Results

Purification and Identification of PIPs by QTAX-Based Tag-Team MS Strategy. The QTAX method (6) is a "TAP"-tag, stable isotope labeling of amino acids in cell culture (SILAC)-based quantitative strategy that uses *in vivo* chemical cross-linking to capture protein complexes and their interacting proteins. It involves two-step affinity purification under fully denaturing conditions using a HBH TAP tag (6, 13). The purified proteins are then identified by LC MS/MS, and the PIPs can be differentiated from background proteins based on their SILAC ratios. Essentially, if a protein is a background protein, it is purified in equal amounts from both the tagged and control strains, and all peptides representing that protein will elute as a pair with a SILAC ratio of ≈1. In contrast, PIPs will be enriched in the tagged sample and have a SILAC ratio >1.5, as shown by coimmunoprecipitation and immunoblot analysis (6).

Previously, we have identified 64 PIPs using tagged Rpn11 alone (6). We also compared the difference in proteasome subunit coverage obtained by using two different baits, Rpn11 and Rpt5, and we noticed there were some obvious differences. For example, the proteasomal component Ecm29 appeared much more abundant in the proteasomes purified from Rpt5-HBH-tagged cells than from Rpn11-HBH-tagged cells. This suggested that some proteins might be differentially enriched after cross-linking due to their spatial location relative to the tagged subunit and/or might be subunit-specific interactions. Therefore, we have now combined QTAX with a team-tag approach to obtain a more comprehensive picture of the proteasome interaction network. We have chosen four unique proteasomal subunits for tagging based on their different spatial locations and functions within the 19S proteasome (14) [Fig. 1*A* and supporting information (SI) Fig. S1]: Rpn11 (subunit of the 19S lid), Rpn10, Rpn1, and Rpt5 (subunits of the 19S base). In addition to the proposed locations, their functions in assisting with the degradation of ubiquitinated substrates have been suggested (3). Rpn11 is a deubiquitinating enzyme and Rpn10 acts as a receptor for ubiquitinated substrates, whereas Rpt5 and Rpn1 have been suggested to be involved in the recognition of ubiquitinated substrates. To quantify all tryptic peptides, the lysine and arginine auxotroph yeast strain (*arg4*Δ *lys2*Δ) expressing a HBH-tagged proteasome subunit was generated for protein purification. To achieve better sensitivity and dynamic range of subsequent MS analysis, sample preparation strategy has been further optimized (*SI Text*). The proteins identified by at least two peptides with a false-positive rate <0.5% were reported here. The SILAC ratios of all tryptic peptides were determined using Search Compare Software (8), manually validated and summarized in Table S1. The SILAC ratios were consistent among biological replicates. By combining the results from all four tagged subunits, a total of 471 putative PIPs (SILAC ratios >1.5) were identified. The number of proteins obtained here is not only substantially more than the 64 PIPs in our previous report (6), but also significantly more than the total of 226 PIPs captured using native affinity purification/MS (4, 5, 9–12). The number of PIPs captured by each bait is as follows: Rpt5–223, Rpn10–299, Rpn1–305, Rpn11–365 (Fig. 1*B*). Of the 471 PIPs, 143 (≈30%) were captured by all four tagged subunits, whereas the rest were captured by using one to three subunits (Tables S2 and S3). Specifically, 131 PIPs were captured with only a single subunit. It is noted that the Rpn11 subunit appears to capture more PIPs than the other three subunits, most likely because of its unique location and function. However, the incorporation of three additional tagged subunits allowed the capture of 106 more PIPs, demonstrating the advantage of the tag-team strategy.

Table 1. List of PIPs captured with high SILAC ratios

GenBank accession no.	Name	No. peptides*	Bait: no. peptides†
YEL037C	Rad23	13	Rpn1:5, Rpn10:5 Rpn11:10, Rpt5:11
YMR276W	Dsk2	3	Rpn11:3
YER143W	Ddi1	3	Rpn11:3
YBR272C	Hsm3	2	Rpt5:2
YDL126C	Cdc48	4	Rpt5:4
YDR006C	Sok1	18	Rpn10:18, Rpn11:7
YOR026W	Bub3	4	Rpn11:4
YHR193C	Egd2	4	Rpn11:4
YLR028C	Ade16	16	Rpn10:16
YIL148W	Rpl40A (Ub)	9	Rpn10:9, Rpn1:7 Rpt5:5, Rpn11:8

*No. of unique peptides with high ratio identified by LC-MS/MS with all baits.
†No. of unique peptides with high ratio identified by LC-MS/MS using each bait.

Categorization of the Identified PIPs. Based on the characteristics of their SILAC ratios, the identified PIPs can be classified into two categories: (*i*) "high" ratio PIPs and (*ii*) defined ratio PIPs. For the first category, the SILAC ratio is "high," because it cannot be calculated due to the lack of detection of a heavy peak in the MS spectra, which indicates these proteins were present only in the tagged sample, similar to the proteasome subunits. The proteins in *i* are summarized in Table 1 and represented by MS spectra in Fig. 2. This group of PIPs includes the Ub-receptor proteins Rad23, Dsk2, and Ddi1, the shuttling factor Cdc48 and ubiquitin. To our knowledge, this is the only study where all known Ub-receptor proteins were captured in a single affinity purification experiment. In addition, five other PIPs have the same characteristic SILAC ratios as the known Ub receptors and proteasome subunits. Although the biological significance of their interactions with the proteasome remains to be explored, we hypothesize that one or

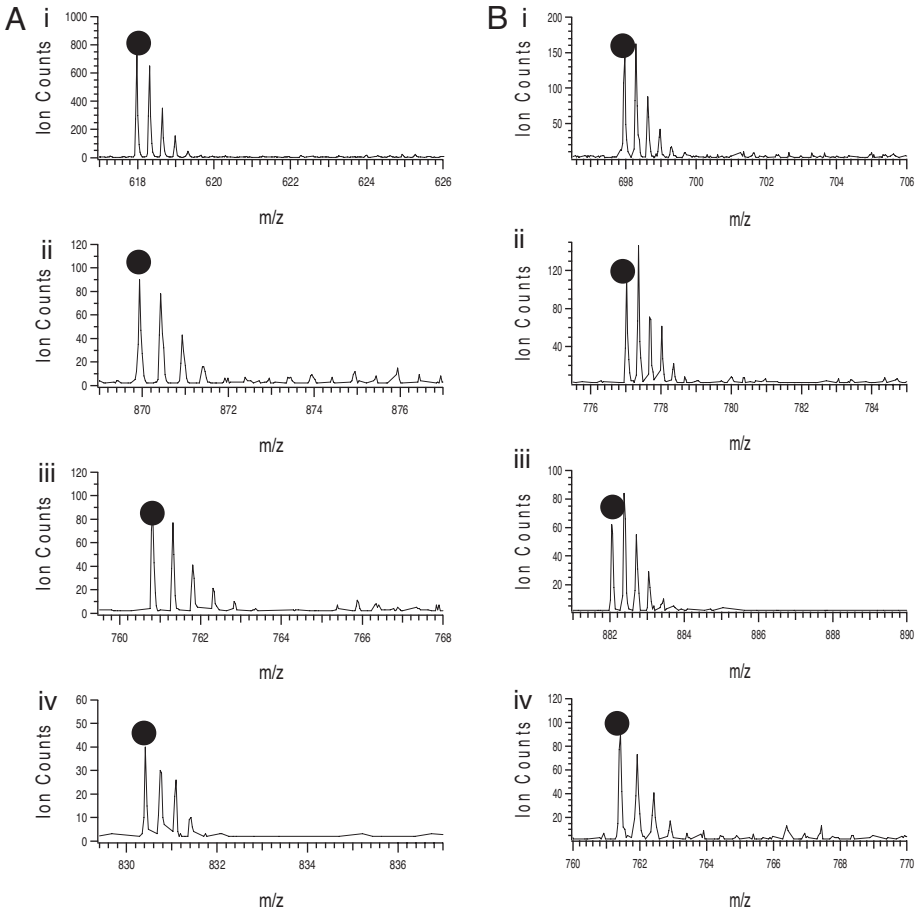

Fig. 2. (*A*) Representative MS spectra of tryptic peptides matched to the four known receptor proteins. (*i*) MH_3^{3+} 617.98, TKVTEPPIAPESATTPGR, matched to Rad23. (*ii*) MH_2^{2+} 869.93, ATQGFSGADLLYIVQR, matched to Cdc48. (*iii*) MH_2^{2+} 760.82, QLNDmGFFDFDR, matched to Dsk2. (*iv*) MH_3^{3+} 617.98, SFQEGLPAPTSVTTSSDKPLTPTK, matched to Ddi1. (*B*) TOF MS spectra of peptides matched to the PIPs with SILAC ratios as high: (*i*) MH_3^{3+} 697.97, VAVEFFDDQGDDYNSSKR, matched to Bub3; (*ii*) MH_3^{3+} 777.02, LAAAQQQAQASGIMPSNEDVATK, matched to Egd2; (*iii*) MH_3^{3+} 882.04, THSGPTTASNPAPSSTNSSSAPSATNSK, matched to Sok1; and (*iv*) MH_2^{2+} 761.43, LFDNNLPYLVSVK, matched to Hsm3. ·, light labeled peptide; o, heavy labeled peptide.

more of these proteins may act as a receptor protein, a proteasome subunit, or a regulator of the proteasome assembly and function.

Among the high-ratio PIPs, Hsm3 is the only one shown to interact with the proteasome by a large-scale yeast TAP/MS study using Hsm3 as the bait (11). Because of its ability to capture the 19S complex, Hsm3 is more likely to be a subunit or a regulator of the proteasome. Sok1 is a high-ratio PIP, which was captured by two baits, Rpn10 and Rpn11. This protein is likely of low abundance in the cell, according to its codon bias value of 0.088, yet it was identified by 18 peptides with high ratios, this protein is interacting specifically with the proteasome. It appears that the Sok1 interaction may be localized near Rpn10 and/or more specific to Rpn10, because the majority of the peptides were captured with the Rpn10 bait. Although no relationship between the proteasome and Sok1 has been reported, in this work, we provide direct evidence to show its physical interaction with the proteasome as described in the validation experiments. Because the proteasome can be regulated by PKA activity (15), and Sok1 has been implicated in cAMP-mediated signaling, their interaction may be biologically important.

Bub3, another high-ratio protein, is a WD40 repeat protein involved in cell-cycle checkpoint regulation that localizes to kinetochores during prophase and metaphase and delays anaphase in the presence of unattached kinetochores (16). There is no previous evidence of a Bub3 interaction with the proteasome, but a genetic interaction between Rad23 and Bub3 has been reported (17). As with Sok1, Bub3 is a low abundant protein, with a 0.018 codon bias value and an estimated 1,430 molecules per cell (www.yeastgenome.org). Because we have captured Bub3 consistently with all peptides having very high ratios, it is likely that it interacts specifically with the proteasome.

The second category includes all proteins that have a defined ratio >1.5. The majority of PIPs (>95%) fall into this category (Table S1), indicating they are enriched in the tagged proteasome sample but not to a complete extent. These proteins represent a broad class of proteins, including members of the translation machinery, transport complexes, metabolic enzymes, and chaperone proteins. It appears the abundance of the PIPs does not correlate with their SILAC ratios, suggesting the ratios are indicators not for protein abundance but rather for their interaction specificity.

Validation of PIPs. Six of the putative PIPs (i.e., Cct4, Hef3, Rvb2, Sec26, Uba1, and Vma13) with different SILAC ratios were chosen for validation by reciprocal copurification and immunoblot analysis. As shown in Fig. 3*A*, all of the PIPs, except Hef3, have been confirmed to interact with the proteasome based on the Western blot using the anti-Rpt1 antibody. Vma13 is a member of the eight-subunit vacuolar H^+-ATPase complex, and five of the other seven subunits were also captured as PIPs. Cct4 is a member of the eight-member cytosolic chaperonin Cct ring complex, and six of the remaining seven subunits were also identified as PIPs in this work. Uba1 is the E1 Ub-activating enzyme. Rvb2 is an essential protein involved in transcription regulation as part of the chromatin remodeling complex. Two of its interacting partners, Rvb1 and Act1, were identified here as PIPs. Sec26 is a subunit of the eight-subunit COPI vesicle coat, and we have captured five subunits of this complex. Hef3 is the translational elongation factor EF-3, the paralog of Yef3. Hef3 interaction with the proteasome was inconclusive based on immunoblot analysis using anti-Rpt1 (Fig. 3*A*). However, Rpt5 was clearly shown to interact with Hef3 by analysis of the same samples with anti-Rpt5 antibody (Fig. 3*B*). Because Hef3 was copurified with the subunits Rpn10, Rpt5, and Rpn11, but

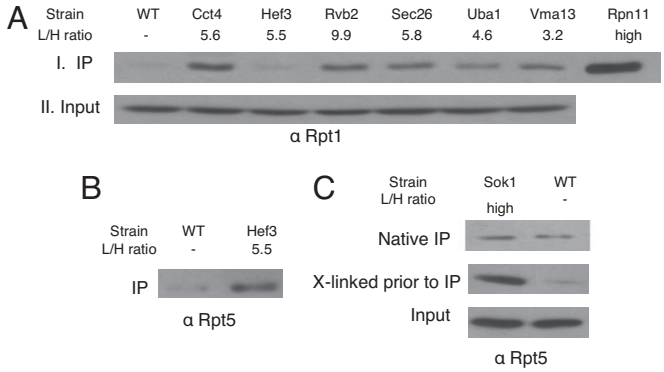

Fig. 3. Validation of the selected PIPs using reciprocal CoIP. (*A*) I. Western blot of native affinity purified samples using anti-Rpt1 from untagged strain (negative control); Cct4-TAP (L/H 5.6); Hef3-TAP (L/H 5.5); Rvb2-TAP (L/H 9.9); Sec26-TAP (L/H 5.8); Uba1-TAP (L/H 4.6); Vma13-TAP (L/H 3.2); Rpn11-TAP (positive control, 1/20 diluted sample loaded). L/H values are the SILAC ratios determined experimentally using Rpn11. II. Comparison of the lysate input used for purification shown in *I*. (*B*) Western blot of the same IP samples used in *A* (*I*) from untagged and Hef3-TAP strains using anti-Rpt5 antibody. (*C*) Validation of Sok1 interaction using Sok1-TAP strain for native purification and Sok1-HBH strain for denaturing purification after *in vivo* formaldehyde cross-linking. The Western blot was obtained using anti-Rpt5.

not with Rpt1, it is possible that Hef3 interacts with a subpopulation of the proteasome complex that is devoid of Rpt1.

To validate one of the high-ratio PIPs, Sok1, we performed a copurification experiment using Sok1-TAP as a bait and immunoblotted against Rpt5. Under native conditions, Sok1 did not copurify with the proteasome (Fig. 3*C*). This was surprising, because Sok1 was clearly identified as a high-ratio PIP. However, reverse copurification without cross-linking under native conditions may not be able to preserve some of the captured interactions by QTAX. Therefore, affinity purification using Sok1-HBH as the bait was carried out under fully denaturing condition after *in vivo* formaldehyde cross-linking, and the Sok1/proteasome interaction was validated (Fig. 3*C*). This result reaffirms that the QTAX strategy is effective in capturing both stable and/or weak/transient protein interactions. A similar observation was reported for RNA polymerase II-interacting proteins when a similar strategy was applied for capturing its interactors by *in vivo* formaldehyde cross-linking and TAP (18).

Protein Interaction Network Analysis. In this study, a large number of putative PIPs were identified with high confidence by QTAX-MS. Because it is not practical to confirm all interactions using copurification and immunoblotting analysis as described above, an alternative strategy is required to better understand the nature of these interactions. Toward this goal, we have performed protein interaction network analysis of the identified PIPs to relate them with previously published protein interaction data. Only the known physical interactions between the identified PIPs and the proteasome subunits and among the identified PIPs were extracted from the interaction databases for our network analyses: in total, 389 of 471 identified PIPs are found to be connected to the proteasome complex either directly or indirectly, whereas 82 PIPs have not been shown to interact with the proteasome and are considered as previously uncharacterized PIPs. A graphic illustration of the protein interaction network consisting of 3,098 interactions among 427 proteins (including the proteasome complex subunits) is displayed in Fig. S2. The majority of PIPs identified in this study (83%) can be placed into the proteasome interaction network based on the known interaction data, supporting the validity of our results. Importantly, no single method has ever captured and identified this scope of proteasome interactions. This result highlights the power of the QTAX-MS approach to comprehensively characterize protein interaction networks.

To correlate the topology in the protein–protein interaction network and the SILAC ratios of PIPs, we have analyzed all of the PIPs captured by Rpn11 as an example. Topology of a PIP is represented by two global topological network properties of the protein in the protein interaction network (Fig. S2): the degree of the node, which is the number of edges incident to the node, and its distance from the proteasome, where the distance of a node is the shortest path length that needs to be traversed from that node to reach any of the proteasome subunits. Intuitively, proteins with higher degrees and/or lower distances from the proteasome in the network imply their higher topological significance. Similarly, higher SILAC ratios imply higher biological significance of the PIPs in the network. As a result, the Pearson correlation analysis suggests a strong correlation between the SILAC ratios of PIPs and their topology in the context of the protein interaction network, meaning that high topological significance implies high biological significance and vice versa, and that topologically similar proteins have similar ratios. This correlation has been further confirmed computationally by using a highly constraining network-topology-based method for grouping proteins in protein interaction networks that belong to the same protein complexes (19). The details of these analyses are presented in *SI Text* and Fig. S3.

Most cellular functions are carried out by protein complexes, and the physical association among protein complexes would suggest their common involvement in a biological function. To categorize the identified interactions into the context of protein complexes and to reveal the interconnectivity of the 26S proteasome complex with other protein complexes, we have extended the network analysis based on the gene ontology (GO) protein complex data available from the *Saccharomyces* Genome Database (SGD) (www.yeastgenome.org). All of the GO protein complexes have defined cellular functions and are known to exist physically *in vivo*. For this analysis, only the complexes with at least 25% of proteins identified by QTAX-MS were included. Aside from the proteasome complex, 154 PIPs were grouped into 35 distinct GO protein complexes (Fig. 4 and Table S4). We also explored the protein interactions among complexes using protein interaction network analysis. If a protein from one complex interacts with another protein in a different complex, an interaction was drawn between the two complexes. As a result, 137 unique interactions among 36 complexes, including the proteasome complex, were mapped, and each interaction between a pair of complexes was weighted by the number of interacting protein pairs between them. Based on the presence of direct interactions between at least one subunit in each complex with one of the proteasome subunits, 19 complexes have been grouped as the first layer interactors, whereas the other 16 complexes appear to connect to the proteasome through their interactions with the first layer interactors and are thus considered as the second layer interactors.

Recently, using the Markov Cluster procedure, Pu *et al.* (20) generated a new description of yeast protein complexes based on high-confidence interaction dataset derived by combining the data from the two latest TAP/MS studies (21). Although the detailed assembly and function of these complexes *in vivo* are not characterized, this dataset represents the most recent and high-confidence categorization of yeast protein complexes based on protein–protein interaction datasets. We performed a similar protein interaction network analysis using the protein complex dataset generated by Pu *et al.* (20), and similar results were obtained (Fig. S4). These results indicate that the QTAX method using *in vivo* chemical cross-linking provides the effective capture of extended interactions of protein complexes.

Discussion

In this work, we present an integrated strategy for a more complete characterization of protein interaction networks and apply the

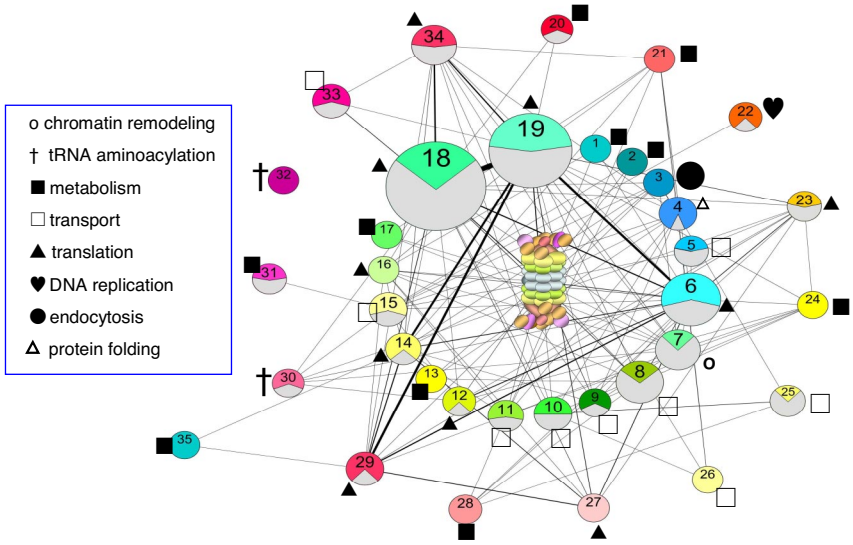

Fig. 4. The interaction map of yeast 26S proteasome with the identified GO complexes (Table S4). The center is the proteasome assembly, and each GO complex is represented as a node. The node size increases as the number of proteins in the complex increase. For non-proteasome complexes, we predict that complexes closer to the center of the figure have a more direct interaction with the proteasome. These data are based on the shortest paths along the interactions in the protein interaction network shown in Fig. S2. The gray color denotes the percentage of proteins of a complex not captured by our study. Interactions between complexes with higher weights (i.e., with more interacting protein pairs among them) are represented with thicker lines. Complex 32 is connected to the proteasome via an identified PIP that is not a member of any GO complex.

strategy to profile the yeast 26S proteasome interaction network. Compared with our previous work (6), several changes have been incorporated into the QTAX strategy for improved peptide analysis. In addition, yeast strains auxotroph for both arginine and lysine (*arg4*Δ *lys2*Δ) were generated to allow quantitation of all tryptic peptides. Combined with these changes, the QTAX-based tag-team approach has proven advantageous for analyzing interaction networks of protein complexes, because the amount of proteins captured with multiple subunits has increased significantly compared with that with a single subunit and is also significantly higher than any of the previous reports. As a result, interacting partners unique to different subunits have been identified, most likely due to their spatial locations to the baits, thus leading to selective enrichment. However, it does not exclude the possibility that some of the captured proteins might be subunit-specific due to the presence of heterogeneous proteasome populations (22). Moreover, validation of the selected PIPs with and without cross-linking has further demonstrated that the QTAX strategy allows capturing protein interactions of all natures. Protein interaction network analysis has been performed by utilizing the known protein interaction data to physically connect the majority of the identified PIPs with the proteasome, further confirming the validity of the identified interacting proteins. This analysis has proven very effective for the comprehensive examination of the 26S proteasome interaction network: a network involving hundreds of proteins intertwined in several critical cellular processes.

One of the advantages of the QTAX strategy is its ability of providing the quantitative ratios for the identified proteins, which have been used for protein categorization. The broad spectrum of PIPs captured may have very diverse functions, and they could be the degradation targets, mediators for assisting protein degradation or the regulators of the proteasome structure and function (3, 15). The higher the SILAC ratios, the more specific interactions the PIPs may have with the bait. There is a group of PIPs with high SILAC ratios similar to the proteasome subunits, including all known Ub-receptor proteins, Rad23, Dsk2, Ddi1, and the shuttling factor Cdc48. Because of the ability to capture all of the known receptors in a single QTAX experiment and the biological significance of these high-ratio proteins, we hypothesize that the rest of proteins with high SILAC ratios in Table 1 are more likely to be directly involved in Ub-proteasome degradation pathway.

In addition to mapping 83% PIPs onto the known yeast proteasome interaction network, protein network analysis has grouped 154 PIPs into 35 GO protein complexes. The proteins within a complex captured by a given proteasome subunit have very similar SILAC ratios. This is not surprising, assuming they interact with the proteasome as a protein complex. These complexes are involved in various biological processes, including chromatin remodeling, tRNA aminoacylation, metabolism, transport, translation, DNA replication, endocytosis, and protein folding. Based on these results, we suspect that the proteasome complex may be implicated in regulating various cellular pathways through its interaction with these complexes. Although the biological significance of most of these interactions remains to be explored, our results provide strong evidence for physical connections between the proteasome and these protein complexes. Among the complexes that have been studied, the chaperonin-containing T complex (Cct complex) is a molecular chaperone that plays important roles in the folding of tubulin, actin, and other cytosolic proteins (23). It is reasonable to propose that Cct interaction with the proteasome facilitates degradation of Cct substrates that failed to be folded correctly. In addition, the Cct complex was suspected to be a substrate of the Ub-proteasome pathway, because Cct complex components accumulated after treatment of proteasome inhibitor (23). However, it is worthwhile to note that recent data have shown that almost all of the identified PIPs did not display changes in abundance in the purified proteasomes upon MG132 treatment (C.G. and L.H., unpublished data). We therefore suspect that the Cct complex more likely functions in assisting protein degradation through its interaction with the proteasome rather than being a substrate itself.

In addition, the proteasome complex is also linked to several translational complexes, including initiation and elongation factor complexes. It has been estimated that up to 50% of newly synthesized protein may be cotranslationally degraded by the proteasome due to errors during translation (24). Because of this, proteasome-mediated cotranslational degradation is an abundant and continuous cellular process. It has been shown that these damaged nascent proteins can be ubiquitinated at the ribosome (25). Interestingly, the Ub-conjugating enzyme Ubc4 (an enzyme lacking significant substrate specificity) is readily detected at the proteasome after translational damage (26). Together, these observations suggest that the proteasome and components of the translational machinery are at a close proximity to each other at sites of translation. Furthermore, the link between protein synthesis and degradation has been demonstrated through the ability of translation elongation factor 1A, eEF1A (Tef1 in yeast) to bind damaged, ubiquitinated nascent proteins and promote their translocation to the proteasome (26). In this study, we have identified subunits of the known

translation initiation and elongation factors in yeast and several ribosomal components as PIPs, consistent with the idea of proteasomes playing a major role in degradation of aberrant translation products.

In summary, our study using the QTAX-based tag-team strategy coupled with protein interaction network analysis provides the most extensive view of the 26S proteasome interaction network to date. We believe the methodology presented here is a valuable and general proteomic tool for the study of protein interaction networks.

Materials and Methods

Strains and Culture Growth/Cross-Linking. Standard yeast growth conditions and media were used. All strains used in this study, except the commercially available TAP-tagged strains (Open Biosystems) are isogenic to 15DaubΔ, bar1Δura3Δns, a derivative of BF264–15D. Rpn11, Rpt5, Rpn10, and Rpn1 were each tagged with the HBH tag at their C-terminal chromosomal locus using a single-step PCR strategy (13). These strains were crossed with an arginine and lysine auxotrophic strain (control), which had been made by deleting *ARG4* with a hygromycine-resistant marker and *LYS2* with a zeocine-resistant marker following a PCR-based strategy. The control strain was grown in heavy media containing $^{13}C_6{}^{15}N_4$-arginine/$^{13}C_6{}^{15}N_2$-lysine, and tagged strains were grown in light media containing $^{12}C_6{}^{14}N_4$-arginine/$^{12}C_6{}^{14}N_2$-lysine, allowing quantification of all tryptic peptides. Cell growth and cross-linking were performed as described (6).

TAP and 2D LC-MS/MS. Purification was carried out similarly as described (6) with the following changes: the lysis buffer contained 8 M urea, 300 mM NaCl, 50 mM NaH_2PO_4, 0.5% Nonidet P-40, 20 mM imidazole, and 1 mM PMSF, pH 8.5. The 20 mM imidazole was added to the lysis and Ni-Sepharose wash buffers to eliminate purification background. In addition, the binding times of both incubation steps have been reduced from overnight to 4 hr to preserve nearly complete specific binding but eliminate nonspecific binding to both resins, because shorter incubation time tends to have less purification background. The combination of these changes has reduced the background significantly and thus allowed improved dynamic range of subsequent MS analysis.

After on-bead trypsin digestion, samples were separated by offline SCX as described, but with a shallower gradient as follows: 0% solvent B (solvent A + 350 mM KCl) to 15% solvent B in 20 min, 15% B to 25% B in 7 min, 25% B to 60%B in 10 min, then 80% B for 5 min. Approximately 20 SCX fractions were collected, desalted using VivaPure C18 microspin columns (Vivascience) and analyzed by 1D LC-MS/MS. Each experiment has been performed in biological replicates.

Database Searching and Data Analysis. The MS analysis was performed by using QSTAR XL MS (Applied Biosystems/PE Sciex), as described (6). The data were searched, using Protein Prospector developmental version 4.25.4, against a normal SGD yeast database concatenated with its randomized version. The proteins were identified by at least two peptides with a false-positive rate $\leq$0.5%. After SILAC ratio [i.e., Light(L)/Heavy(H)] determination using Search Compare, manual ratio validation was carried out when the SILAC ratio standard deviation of an identified protein was >30% or the proteins identified by only two or three peptides. Details are in *SI Text*.

Validation of Selected PIPs. Reverse copurification using yeast strains expressing TAP-tagged proteins (i.e., the selected PIPs) and immunoblot analysis were carried out as described (6), except with the following buffers: lysis/wash buffer contained 25 mM Tris·HCl, pH 8.0; 200 mM NaCl; 5 mM EDTA; 10% glycerol; 0.5% Nonidet P-40; protease and phosphatase inhibitors. TEV cleavage buffer contained 50 mM Tris·HCl, pH 8.0; 10% glycerol; 0.5 mM EDTA; 1% Triton; 1 mM DTT.

Protein Interaction Network Analysis. To construct protein interaction networks, we used protein interaction data from the following databases and studies: BioGRID (www.thebiogrid.com), MIPS (http://mips.gsf.de), and a recently published, high-confidence yeast protein interaction dataset (21). The number of physical protein interactions in BioGRID is 31,687, and they occur among 4,656 proteins. The number of physical interactions in MIPS is 7,385, and they occur among 4,223 proteins. We have constructed the protein interaction network based on the following physical interactions from these datasets to filter the dataset for physical interaction and exclude interactions based on colocalization and similar approaches: affinity capture (MS and Western blot analysis), coimmunoprecipitation, two-hybrid, reconstituted complex, cocrystal structure, FRET, far-Western blot analysis, and surface plasma resonance. Finally, we use interactions described by Collins *et al.* (21) having a confidence level >0.38, resulting in protein interaction data containing 12,035 interactions among 1,921 proteins. We choose a threshold of 0.38, because these interactions are of high confidence. We later extended the analysis to complexes defined by Pu *et al.* (20), where the same threshold was used to construct protein complexes.

ACKNOWLEDGMENTS. We thank Prof. A. L. Burlingame, Peter Baker, and Aenoch Lynn (University of California, San Francisco) for the use of Protein Prospector; Yingying Yang (University of California, Irvine) for yeast strains; Marija Rašajski (University of California, Irvine) for help with the initial Venn diagram; Dr. Jeff Jones (University of California, Irvine) for help with the initial ratio analysis; and members of the Huang and Kaiser laboratories for help during this study. This work was supported by National Institutes of Health Grants GM-74830 (to L.H.) and GM-66164 (to P.K.), by the Department of the Army (Grant PC-041126, to L.H.), and by National Science Foundation CAREER Grant IIS-0644424 (to N.P.).

1. Alberts B (1998) The cell as a collection of protein machines:preparing the next generation of molecular biologists. *Cell* 92:291–294.
2. Pickart CM, Cohen RE (2004) Proteasomes and their kin: Proteases in the machine age. *Nat Rev Mol Cell Biol* 5:177–187.
3. Schmidt M, Hanna J, Elsasser S, Finley D (2005) Proteasome-associated proteins: regulation of a proteolytic machine. *Biol Chem* 386:725–737.
4. Verma R, *et al.* (2000) Proteasomal proteomics: Identification of nucleotide-sensitive proteasome-interacting proteins by mass spectrometric analysis of affinity-purified proteasomes. *Mol Biol Cell* 11:3425–3439.
5. Leggett DS, *et al.* (2002) Multiple associated proteins regulate proteasome structure and function. *Mol Cell* 10:495–507.
6. Guerrero C, Tagwerker C, Kaiser P, Huang L (2006) An integrated mass spectrometry-based proteomic approach: Quantitative analysis of tandem affinity-purified *in vivo* cross-linked protein complexes (QTAX) to decipher the 26 S proteasome-interacting network. *Mol Cell Proteom* 5:366–378.
7. Wang X, *et al.* (2007) Mass spectrometric characterization of the affinity-purified human 26S proteasome complex. *Biochemistry* 46:3553–3565.
8. Wang X, Huang L (2008) Identifying dynamic interactors of protein complexes by quantitative mass spectrometry. *Mol Cell Proteomics* 7:46–57.
9. Gavin A, *et al.* (2002) Functional organization of the yeast proteome by systematic analysis of protein complexes. *Nature* 415:141–147.
10. Ho Y, *et.al.* (2002) Systematic identification of protein complexes in Saccharomyces cerevisiae by mass spectrometry. *Nature* 415:180–183.
11. Gavin AC, *et al.* (2006) Proteome survey reveals modularity of the yeast cell machinery. *Nature* 440:631–636.
12. Krogan NJ, *et al.* (2006) Global landscape of protein complexes in the yeast *Saccharomyces cerevisiae. Nature* 440:637–643.
13. Tagwerker C, *et al.* (2006) A tandem affinity tag for two-step purification under fully denaturing conditions: Application in ubiquitin profiling and protein complex identification combined with *in vivo*cross-linking. *Mol Cell Proteom* 5:737–748.
14. Sharon M, *et al.* (2006) Structural organization of the 19S proteasome lid: Insights from MS of intact complexes. *PLoS Biol* 4:e267.
15. Gomes AV, *et al.* (2006) Mapping the murine cardiac 26S proteasome complexes. *Circ Res* 99:362–371.
16. Martinez-Exposito MJ, Kaplan KB, Copeland J, Sorger PK (1999) Retention of the BUB3 checkpoint protein on lagging chromosomes. *Proc Natl Acad Sci USA* 96:8493–8498.
17. Collins SR, *et al.* (2007) Functional dissection of protein complexes involved in yeast chromosome biology using a genetic interaction map. *Nature* 446:806–810.
18. Tardiff DF, Abruzzi KC, Rosbash M (2007) Protein characterization of Saccharomyces cerevisiae RNA polymerase II after *in vivo* cross-linking. *Proc Natl Acad Sci USA* 104:19948–19953.
19. Milenkovic T, Przulj N (2008) Uncovering biological network function via graphlet degree signatures. *Cancer Inform* 6:257–273.
20. Pu S, *et al.* (2007) Identifying functional modules in the physical interactome of *Saccharomyces cerevisiae. Proteomics* 7:944–960.
21. Collins SR, *et al.* (2007) Toward a comprehensive atlas of the physical interactome of *Saccharomyces cerevisiae. Mol Cell Proteom* 6:439–450.
22. Drews O, *et al.* (2007) Mammalian proteasome subpopulations with distinct molecular compositions and proteolytic activities. *Mol Cell Proteom* 6:2021–2031.
23. Yokota S, *et al.* (2000) Proteasome-dependent degradation of cytosolic chaperonin CCT. *Biochem Biophys Res Commun* 279:712–717.
24. Reits EA, Vos JC, Gromme M, Neefjes J (2000) The major substrates for TAP *in vivo* are derived from newly synthesized proteins. *Nature* 404:774–778.
25. Zhou M, Fisher EA, Ginsberg HN (1998) Regulated co-translational ubiquitination of apolipoprotein B100. A new paradigm for proteasomal degradation of a secretory protein. *J Biol Chem* 273:24649–24653.
26. Chuang SM, *et al.* (2005) Proteasome-mediated degradation of cotranslationally damaged proteins involves translation elongation factor 1A. *Mol Cell Biol* 25:403–413.